Results

Swelling of astrocytic cell processes, perivascular end-feet, and cell body had already begun 15 min after the ischemic insult, without accumulation of glycogen granules [12]. At this stage, isolated dark neurons with diffuse, increased electron density were found disseminated among the almost normal-looking neurons. Some of the normal-appearing neurons showed disaggregated ribosomes and slight swelling of the rough endoplasmic reticulum (rER) and Golgi apparatus. The swollen astrocytic cell processes surrounded these dark neurons. Small dots of chromatin condensation were observed scattered in the nuclear matrix as well as along the nuclear membrane of the dark neurons. However, no swelling was observed in mitochondria and the other cytosolic organelles. These dark neurons were never found in the control animals after the same procedures for fixation and preparation as used for the postischemic animals.

From 5 to 24 h, isolated dark neurons with different grades of high electron density increased in number among the almost normal looking neurons (Fig. 1 d), some of which showed disaggregation of ribosomes and slight swelling of their rER and Golgi apparatuses as seen at 15 min. These dark neurons still newly appeared even 3 weeks after the start of recirculation. In the swollen astrocytic cell processes, enlarged mitochondria having slightly swollen cristae and boosted electron density of the matrices had increased in number, together with increased accumulation of glycogen granules [12, 13]. These dark neurons were compatible with ischemic neuronal change seen by HE staining. These ischemic neurons were scattered among the normal-looking neurons in the ischemic penumbra of the cerebral cortex, and had a homogeneous eosinophilic cytosol containing a pycnotic and/or karyorrhectic nucleus (Fig. 2 a) [10]. In this stage, TUNEL-positive nuclei showing strong positively on the dotted chromatin condensations of the neuron were also observed scattered in the ischemic penumbra of the cerebral cortex (Fig. 2 b). The dark neurons were surrounded by remarkably swollen astrocytic cell processes, especially prominent nearby the dendritic synapses of the dark neurons [31] (Fig. 1 c), and showed darkened nuclei in which dots of chromatin condensates were observed (Fig. 1 b). Later than 12 h after the ischemic insult, some mitochondria of these dark neurons showed partial swelling of their matrices and disintegration of cristae with woolly densities (Fig. 1 a). Among these dark neurons, completely shrunken neurons surrounded by remarkably swollen astrocytic cell processes (Fig. 1 c) were increased in number from 12 to 24 h after the ischemic insult. These shrunken neurons often contained mitochondria with swollen matrices having woolly densities.

By 4 days after the ischemic insult, these shrunken neurons were fragmented by astrocytic cell processes that had invaded and separated the shrunken neuronal cytosol and nucleus. Up to this stage, no inflammatory cells and macrophages appeared in the ischemic penumbra. However, phagocytic activity of the perivascular microglia was observed.

Fig. 1 a–d. Electron microscopy of electron dense dying neurons: **a** Later than 12 h after the ischemic insult, some mitochondria of these dark neurons shows partial swelling of their matrices and disintegration of cristae with woolly densities (arrows) (×6000); **b** the dark neuron shows darkened nucleus (N) in which dots of chromatin condensates are observed. Nuclear membrane is swollen and disintegrated (×4000); **c** two dark neurons with different grade of electron density are surrounded by remarkably swollen astrocytic cell processes, especially prominent nearby the dendritic synapses of the dark neurons. N: nucleus (×1500); **d** twelve hours after ischemic insult, isolated dark neurons with different grades of high electron density increased in number among the almost normal looking neurons (×500)

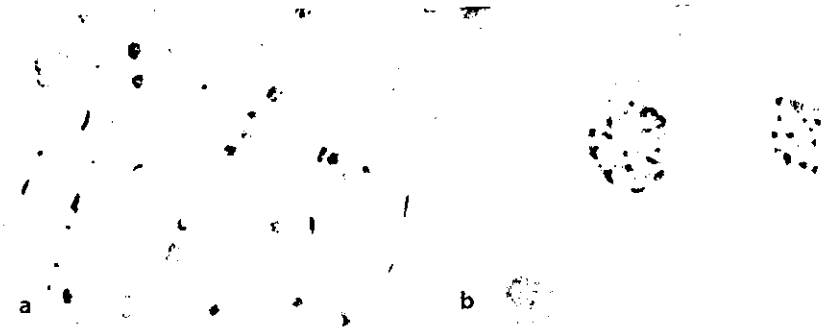

Fig. 2a, b. Light microscopy of neurons showing eosinophilic ischemic change: **a** the ischemic neurons are scattered among the normal-looking neurons in the ischemic penumbra of the cerebral cortex, and have a homogeneous eosinophilic cytosol containing a pycnotic and/or karyorrhectic nucleus (H.E. ×400); **b** TUNEL-positive nuclei showing strong positivity on the dotted chromatin condensations of the neuron are observed scattered in the ischemic penumbra of the cerebral cortex (TUNEL ×800)

Discussion

Kerr and Wyllie (1972) [15] found apoptosis after a mild ischemic insult to the liver cells; i.e., as the isolated cell died, the nucleus became condensed with large crescent-shaped chromatin condensates and fragmented into separate pieces, the condensed cytosol was also fragmented into separate apoptotic bodies containing fragmented nuclear material and normal cytosolic organelles; and these apoptotic bodies were phagocytized by macrophages. While, in necrosis, not isolated but a massive number of cells die with swollen cytosol and organelles; and the nucleus is also swollen with small chromatin condensates. Finally all cellular and nuclear membranes are ruptured. As some neurons die isolatedly with cellular condensation after a mild ischemic insult to the brain, the possibility of apoptotic neuronal death has been discussed.

The present study was aimed at elucidating time course of the ultrastructural morphological changes occurring in isolated cells undergoing neuronal death in the cerebral cortex with special regard to the behavior of the surrounding astrocytic cell processes after a mild ischemic insult, in order to discuss better the topic of apoptosis vs. necrosis for the neuronal death.

In the present model, post ischemic injuries mature slowly in the cerebral cortex. The temporal profile of histopathology revealed the development of disseminated selective neuronal necrosis (DSNN) only in the penumbra area of the cerebral cortex after the ischemic insult. However, in the infarcted focus of the frontal lobe, following temporary development of DSNN, all neurons and astrocytes except for the capillary wall itself undergo massive necrosis with marked swelling and destruction of the entire membranous system of the cells [10–12, 22].

In the penumbra, under EMS observation, the DSNN appeared from the early post ischemic stage at 15 min after the start of recirculation, as isolated dark neurons with different grades of high electron density of their cytosol and nucleus. In these dark neurons, no swelling of mitochondria and other cytosolic organelles

was observed, except in shrunken neurons with very high electron density of the entire cell. As the dark neuron showed small loosely aggregated chromatin condensates scattered in the nuclear matrix as well as along the nuclear membrane, cellular activity had probably decreased [22]. These isolated dark neurons with different grades of electron density increased in number from 5 min to 24 h, and were still newly appeared 3 weeks after the ischemic insult.

The astrocytic cell bodies and processes were remarkably swollen, especially those nearby the dendritic synapses of the dark neurons; their mitochondria increased in number and size; and they accumulated glycogen granules from 5 to 24 h after the ischemic insult. These astrocytic mitochondria showed moderately swollen cristae and increased electron densities of their matrices [12, 13]. These findings highly suggest activated astrocytic energy metabolism, generating lactate as a neuronal fuel [2, 6], scavenging potassium [25], neurotransmitters [19, 24], and other metabolites from the neuron and dendritic synapses, and also promoting survival of the astrocytes themselves [18]. As the neuronal fuel would not be transferred smoothly to neurons due to deranged neuronal energy metabolism, glycogen would accumulate in the astrocytic cell processes via gluco-neogenesis from lactate followed by glycogenesis [3, 6, 28–30].

Among the dark neurons with increased electron density, completely shrunken neurons with very high electron density of the entire cell body and axons increased in number from 5 to 24 h after the ischemic insult. Later than 12 h after the ischemic insult, some mitochondria of the isolated dark neurons showed partial swelling of their matrices, and disintegrated cristae with woolly densities. However, many of the mitochondria in the shrunken neurons showed swollen matrices with occasional woolly densities and disintegrated cristae; and such cells were considered to irreversibly damaged and unable to survive [5]. From our findings, not every dark neuron died to become a shrunken neuron, but some of them survived. Further quantitative study of the fate of these isolated dark neuron is necessary.

Four days after the ischemic insult, these condensed neuronal bodies became separated and fragmented by invasion of tiny astrocytic cell processes. Some of these fragments were phagocytized by astrocytic cell processes, and others were seen moving in the intercellular spaces. No inflammatory cells or phagocytes were seen in this study. Only the perivascular microglia showed phagocytic activities. Our present study suggests that the astrocytic cell processes around the dark neuron reacted to rescue the injured neuron by generating fuels, scavenging neuronal and synaptic metabolites [14, 16, 19, 25, 27, 30] and disposed dead neurons by shrinking, smashing and phagocitizing them.

Necrosis versus apoptosis in ischemic neuronal death has been controversial. In the present study, some of the morphological findings on the dark neurons indicated classical necrosis: i.e., on eosinophilic ghosting of cells in terms of histology; small loose aggregates of nuclear chromatin in the nuclear matrix and margin, instead of the marginates of condensed coarse granular aggregates seen in apoptosis; and a lack of apoptotic bodies. Others corresponded to apoptosis: scattered individual cells affected in terms of histology (shrinkage necrosis); lack of exudative inflammation, and condensation of the cytosol with structurally intact mitochondria and other organelles, instead of swelling of all cell component followed by

rupture of cell membrane and destruction of cytosolic organelles as seen in necrosis [21, 33]. But, sometimes dead cells are swollen and sometimes they are shrunken depending on the cellular environment [21]. In the ischemic penumbra, swollen perineuronal astrocytes seemed to cause condensation of the necrotic neuron, resulting in shrinkage. While, when astrocytes died in the infarcted area, all neurons and astrocytes swelled and all of their membrane systems were ruptured. The macrophage seemed not to be able to enter the intact neuropils like those in the penumbra, but could enter the infarct focus where neuropils have been disrupted.

Conclusion

In conclusion: 1) The ultrastructural characteristics of DSNN, in the present study, suggested necrotic neuronal death instead of apoptosis. Condensation of the isolated neuron was induced by swelling of astrocytic cell processes surrounding the dark neuron. 2) Nuclear chromatin condensations observed from the early stage in appearance of the dark neurons indicated an initiating factor of the neuronal derangement. As the TUNEL procedure resulted in staining at the nuclear chromatin condensates of the dark neuron, in the present study, some DNA derangement seemed to be involved in this process [20, 32]. Further ultrastructural TUNEL staining is necessary to determine the ultrastructural characteristics of the TUNEL-positive neurons. 3) Not all dark neurons seems to die, but some of them to survive. Mitochondrial dysfunction seemed to be a determining factor of the irreversibility.

References

1. Colbourne F, Sutherland GR, Auer RN (1999) Electron microscopic evidence against apoptosis as the mechanism of neuronal death in global ischemia. J Neurosci 19(11):4200–4210
2. Coles JA (1995) Glial cells and the supply of substrates of energy metabolism to neurons. In: Kettenmann H, Ransom B (eds) Neuroglia. Oxford University Press, New York Oxford, pp 793–804
3. Dringen R, Schmoll D, Cesar M, Hamprecht B (1993) Incorporation of radioactivity from [14C] lactate into the glycogen of cultured mouse astroglial cells. Evidence for gluconeogenesis in brain cells. Biol Chem Hoppe Seyler 374(5):343–347
4. Dux E, Oschlies U, Uto A, Kusumoto M, Hossmann KA (1996) Early ultrastructural changes after brief histotoxic hypoxia in cultured cortical and hippocampal CA1 neurons. Acta Neuropathol (Berl) 92(6):541–544
5. Ghadially FN (1997) Ultrastructural Pathology of the Cell and Matrix, 4th edn. Butterworth-Heinemann 18–29:246–258
6. Hamprecht B, Dringen R (1995) Energy metabolism. In: Kettenmann H, Ransom B (eds) Neuroglia. Oxford University Press, New York Oxford, pp 473–487
7. Hanyu S, Ito U, Hakamata Y, Yoshida M (1995) Transition from ischemic neuronal necrosis to infarction in repeated ischemia. Brain Research 686:44–48
8. Hanyu S, Ito U, Hakamata Y, Nakano I (1997) Topographical analysis of cortical neuronal loss associated with disseminated selective neuronal necrosis and infarction after repeated ischemia. Brain Res 767(1):154–157
9. Ito U, Hanyu S, Hakamata Y, Kuroiwa T, Yoshida M (1997) Features and threshold of infarct development in ischemic maturation phenomenon. In: Ito U, Kirino T, Kuroiwa T, Klatzo I (eds) Maturation Phenomenon in Cerebral Ischemia II. Springer, Berlin Heidelberg, pp 115–121
10. Ito U, Hanyu S, Hakamata Y, Arima K, Oyanagi K, Kuroiwa T, Nakano I (1999) Temporal profile of cortical injury following ischemic insult just-below and at the threshold level for induc-

tion of infarction: light and electron microscopic study. In: Ito U, Orzi F, Kuroiwa T, Fieschi C, Klatzo I (eds) Maturation Phenomenon in Cerebral Ischemia III. Springer, Berlin Heidelberg, pp 227–235
11. Ito U, Spatz M, Walker J Jr, Klatzo I (1975) Cerebral ischemia in mongolian gerbils. I. Light microscopic observations. Acta Neuropathol Berl 32(3):209–223
12. Ito U, Kuroiwa T, Hanyu S, Hakamata Y, Arima K, Oyanagi K, Nakano I (1999) Ultrastructural features of astroglial mitochondria following temporary ischemia at threshold level to induce infarction. In: Krieglstein J (ed) Pharmacology of cerebral ischemia. medpharm Science Publication, Stuttgart, pp 113–117
13. Ito U, Kuroiwa T, Hanyu S, Hakamata Y, Arima K, Oyanagi K, Nakano I (2000) Ultrastructure and morphometry of astroglial mitochondria following temporary threshold ischemia to induce focal infarction. In: Bazan NG, Ito U, Kuroiwa T, Klatzo I (eds) Maturation Phenomenon in Cerebral Ischemia IV. Springer, Berlin Heidelberg, pp 253–259
14. Kempski O, Volk C (1997) Glial protection against neuronal damage. In: Ito U, Kirino T, Kuroiwa T, Klatzo I (eds) Maturation Phenomenon in Cerebral Ischemia II. Springer, Berlin Heidelberg, pp 115–121
15. Kerr JF, Wyllie AH, Currie AR (1972) Apoptosis: a basic biological phenomenon with wide-ranging implications in tissue kinetics. Br J Cancer 26(4):239–257
16. Kimelberg HK, Rutledge E, Goderie S, Charniga C (1995) Astrocytic swelling due to hypotonic or high K+ medium causes inhibition of glutamate and aspartate uptake and increases their release. J Cereb Blood Flow Metab 15(3):409–416
17. Kirino T (1982) Delayed neuronal death in the gerbil hippocampus following ischemia. Brain Res 239(1):57–69
18. Kraig RP, Lascola CD, Caggiano A (1995) Glial response to brain ischemia. In: Kettenmann H, Ransom B (eds) Neuroglia. Oxford University Press, New York Oxford, pp 964–976
19. Levi G, Gallo V (1995) Release of neuroactive amino acids from glia. In: Kettenmann H, Ransom B (eds) Neuroglia. Oxford University Press, New York Oxford, pp 815–826
20. Li PA, Rasquinha I, He QP, Siesjo BK, Csiszar K, Boyd CD, MacManus JP (2001) Hyperglycemia enhances DNA fragmentation after transient cerebral ischemia. J Cereb Blood Flow Metab 21(5):568–576
21. Majno G, Joris I (1995) Apoptosis, oncosis, and necrosis. An overview of cell death. Am J Pathol 146(1):3–15
22. Marcoux FW, Morawetz RB, Crowell RM, DeGirolami U, Halsey JH Jr (1982) Differential regional vulnerability in transient focal cerebral ischemia. Stroke 13(3):339–346
23. Martin LJ (2001) Neuronal cell death in nervous system development, disease, and injury (Review). Int J Mol Med 7(5):455–478
24. Martin DL (1995) The role of glia in the inactivation of neurotransmitters. In: Kettenmann H, Ransom B (eds) Neuroglia. Oxford University Press, New York Oxford, pp 732–745
25. Newman EA (1995) Glial cell regulation of extracellular potassium. In: Kettenmann H, Ransom B (eds) Neuroglia. Oxford University Press, New York Oxford, pp 717–731
26. Ohno K, Ito U, Inaba Y (1984) Regional cerebral blood flow and stroke index after left carotid artery ligation in the conscious gerbil. Brain Res 297(1):151–157
27. Rosenberg GA, Aizeman E (1989) Hundred-fold increase in neuronal vulnerability to glutamate toxicity in astrocyte-poor cultures of rat cerebral cortex. Neuroscience Letters 103:162–168
28. Sokoloff L (1992) Energy metabolism and effects of energy depletion or exposure to glutamate. Can J Physiol Pharmacol 70(12):S107–112
29. Sokoloff L, Gotoh J, Law MJ, Takahashi S (1996) Functional activation of energy metabolism in brain tissue: Roles of neurons and astroglia. In: Krieglstein J (ed) Pharmacology of cerebral ischemia. medpharm Scientific Publ, Stuttgart, pp 259–270
30. Swanson RA, Choi DW (1993) Glial glycogen stores affect neuronal survival during glucose deprivation in vitro. J Cereb Blood Flow Metab 13(1):162–169
31. von-Lubitz DK, Diemer NH (1983) Cerebral ischemia in the rat: ultrastructural and morphometric analysis of synapses in stratum radiatum of the hippocampal CA-1 region. Acta Neuropathol Berl 61(1):52–60
32. Wijsman JH, Jonker RR, Keijzer R, van de Velde CJ, Cornelisse CJ, van Dierendonck JH (1993) A new method to detect apoptosis in paraffin sections: in situ end-labeling of fragmented DNA. J Histochem Cytochem 41(1):7–12
33. Wyllie AH, Kerr JF, Currie AR (1980) Cell death: the significance of apoptosis. Int Rev Cytol 68:251–306

Amyotrophic lateral sclerosis: On the origin of the degenerated fibers in the white matter of the spinal cord

Kiyomitsu Oyanagi, Mineo Yamazaki, Emiko Kawakami, Takashi Morita, Takao Makifuchi, Hitoshi Takahashi

Running title: Origin of degenerated fibers in ALS spinal cord

Kiyomitsu Oyanagi, Mineo Yamazaki and Emiko Kawakami

Department of Neuropathology, Tokyo Metropolitan Institute for Neuroscience, Tokyo, Japan

Mineo Yamazaki

Department of Neurology, Nippon Medical University, Tokyo, Japan

Takashi Morita

Department of Pathology, Shinrakuen Hospital, Niigata, Japan

Takao Makifuchi

Department of Neuropathology, National Saigata Hospital, Niigata, Japan

Hitoshi Takahashi

Department of Pathology, Brain Research Institute, Niigata University, Niigata, Japan

*Correspondence to: Kiyomitsu Oyanagi, MD, PhD, Department of Neuropathology, Tokyo Metropolitan Institute for Neuroscience,
2-6 Musashidai, Fuchu, Tokyo 183-8526, Japan
Tel.: +81-42-325-3881 Ext. 4711, Fax: +81-42-321-8678,
e-mail: k123ysm@tmin.ac.jp

Abstract

The characters of the degeneration of the white matter of the spinal cord of amyotrophic lateral sclerosis (ALS) were examined, and the origins of the degenerated fibers were discussed.

1. The degree of large myelinated fiber loss in the lateral corticospinal tract (l-CST) did not correlate with either the duration of their illness or their history of respirator use. Direct correlation of disease mechanism was absent between the anterior horn cells and the l-CST in classic ALS.

2. The patients who required respirator support showed more severe degeneration of the anterolateral funiculus (ALF) in the ALS than those who required none. The large myelinated fibers in the l-CST and ALF degenerate independently in classic ALS.

3. The large myelinated fibers in the ALF of the mid-cervical spinal cord of humans originate from the tegmentum of the brain stem and the lower cervical spinal cord, not from the cerebrum, or the thoracic or lumbar spinal cord. The origin of the large myelinated fibers in the ALF of the spinal cord in humans, is considered to be the long-descending neurons in the brain stem tegmentum and the propriospinal neurons in the spinal cord.

Key words: Amyotrophic lateral sclerosis, Anterolateral funiculus, Corticospinal tract, Middle root zone, Morphometry, Spinal neurons

INTRODUCTION

Amyotrophic lateral sclerosis (ALS) is a motor neuron disease occurring in adults mainly involving the upper and lower motor neurons with relative sparing of the abducens and oculomotor nerve nuclei, and of the autonomic and sensory neurons in the brain stem and spinal cord. About 90% of ALS patients have been reported to be sporadic, and the sporadic ALS are roughly classified into classic ALS, "multi-system type ALS" [Hayashi & Kato 1989, Mizutani et al. 1992], and ALS with temporal lobe involvement [Yuasa 1970, Mitsuyama & Takamatsu 1971, Nakano et al. 1992]. Among the familial ALS patients, superoxide dismutase (SOD)-1 gene mutation was revealed in about 20% of the patients [Shaw 2001].

In the spinal cord of ALS, degeneration of the corticospinal tract (CST), lateral and anterior, is commonly obvious. In addition to this, since being proposed by Charcot [1880], it has been reported repeatedly that degeneration of the anterolateral funiculus (ALF) occurs in the spinal cord of patients with classic ALS (Fig. 1) [Holmes 1909, Ikuta et al. 1979, 1982, Lawyer & Netsky 1953, Smith 1960]. The posterior funiculus was scarcely/occasionally involved in the classic ALS, but severely deteriorated in the "multi-system type ALS" [Hayashi & Kato 1989, Mizutani et al. 1992]. Some cases of familial ALS with or without superoxide dismutase (SOD)-1 mutation show degeneration of the posterior funiculus and spinocerebellar and spinothalamic tracts in addition to the CST degeneration.

In the present paper, the characteristic patterns of the degeneration of the white matter of the spinal cord of ALS patients were analyzed, and the origins of the

degenerated fibers was discussed, based on the observation by the authors and the literature review.

MATERIALS AND METHODS

1. Examined subjects

The control subjects and patients with sporadic and familial ALS examined by the authors were Japanese, and none of them had had cardiac arrest, hypoglycemic episodes, or severe liver dysfunction. Neuropathological findings of many of the cases were previously reported by the authors [Ikuta et al. 1979, 1982, Makifuchi & Ikuta 1977, Oyanagi et al. 1983, 1989, 1995, 1999, Takahashi et al. 1992, 1993a, 1993b, 1994].

2. Light microscopic examination

Serial 6-μm-thick sections of the brains and spinal cords were made from 10% formalin- or 4 % paraformaldehyde in phosphate buffer-fixed-paraffin embedded blocks, and stained with hematoxylin-eosin, Klüver-Barrera, Bodian, Gallyas, phosphotungustic acid hematoxylin, periodic acid Schiff and other preparations, and examined light microscopically. Other sections (also 6 μm thick) were subjected to immunohistochemical staining using the avidin-biotin-peroxidase complex (ABC) method, using a Vectastain ABC kit (Vector, Burlingame, CA, USA). The primary antibodies used were: rabbit anti-cow ubiquitin polyclonal antibody (dilution 1:150; Dakopatts A/S, Glostrup, Denmark), a rabbit anti-cystatin C (dilution 1:1000; DAKO, Denmark), a rabbit anti-Cu/Zn superoxide dismutase (SOD; dilution 1:10000, a gift from Dr. K.

Asayama, Yamanashi Medical School, Yamanashi, Japan), a mouse anti-phosphorylated neurofilament protein (SMI-31; dilution 1:10000, Sternberger Monoclonals, Baltimore, Md, USA), a rabbit anti-glial fibrillary acidic protein (GFAP) polyclonal antibody (dilution 1:500; Dakopatts A/S, Glostrup, Denmark), rabbit anti-human tau polyclonal antibody [dilution 1:1000; a gift from Prof. Y. Ihara, Tokyo University, Tokyo, Japan], anti-tau monoclonal antibody AT8 (dilution 1:1000) (Innogenetics, Belgium), and anti-α-synuclein monoclonal antibody LB509 [gift from Prof. T. Iwatsubo, Tokyo University, Tokyo, Japan]. Antigenicity was increased for ubiquitin immunostaining by pretreating the sections with 0.025% trypsin for 15 min at room temperature, and for α-synuclein immunohistochemistry by pretreating the sections with hydrated autoclaving (121°C, 15 min). Nonspecific binding of the biotin/avidin system reagents was blocked by pretreating the sections with a blocking solution from the kit (Vector), and then incubating them with the required primary antibody overnight at 4°C. The sections were then incubated with the secondary reagent containing biotinylated anti-rabbit, or anti-mouse IgG (diluted 1:200) for 2 h, and finally with the ABC solution for 1 h. The sections were subjected to the peroxidase reaction using freshly prepared 0.02% 3,3'-diaminobenzidine-tetrahydrochloride and 0.005% hydrogen peroxide in 0.05 M Tris-HCl buffer, pH 7.6, for 10 min at room temperature. As antibody controls, the primary antisera were either omitted or were replaced with normal rabbit or mouse serum. Several specimens of neural and non-neural tissue from the patients served as positive or negative tissue controls.

3. Topographic and quantitative study of the neurons in the spinal cord

Tissues were embedded in paraffin, serially sectioned at 8 μm, and stained with thionine. The thickness of the sections was verified by manipulating the fine adjustment drum of the light microscope. Five serial sections each of the 5th cervical and of the 7th thoracic segment and 4 serial sections of the second sacral segment were examined. The entire spinal gray matter of each serial section was surveyed under 1000-fold magnification. Neurons were identified by the presence of Nissl substance and prominent nucleoli. The longest diameter of the nucleus (A) and the largest dimension perpendicular to the diameter (B) were measured with an ocular micrometer (4), and the nuclear area (S) was calculated according to the formula $S=\pi AB/4$. There was a significant positive correlation coefficient ($r=0.97$) between the area obtained by calculation and that obtained by counting 1 mm squares of section paper over the enlarged photograph of the nuclei.

The frequency distribution of nuclear areas by 10 μm^2 increments was obtained for each case, and it was represented in graphs as the nuclear area x n (number of nuclei) to show that the large nuclei, though fewer in number, cover a wider area.

Spinal neurons were classified into 14 groups according to their nuclear areas. The first group was composed of neurons whose nuclear areas were smaller than 40 μm^2. Neurons with nuclear area ranging from 41 to 150 μm^2 were divided into 11 groups (2nd to 12th) in 10 μm^2 increments. The 13th group consisted of neurons with nuclear areas of 151 to 200 μm^2, and the 14th, neurons with nuclear areas greater than 201 μm^2. Each of the neurons was expressed by dots of various sizes and was plotted on the trace of the spinal gray matter magnified 100 times.

4. Quantitative examination of the myelinated fibers in the lateral corticospinal tract (l-CST) and anterolateral funiculus (ALF) of the spinal cord

The fourth or fifth cervical segments of the spinal cord were fixed in 20% formalin in 0.1 M phosphate buffer (PB; pH 7.3) or 3% glutaraldehyde-1% paraformaldehyde in 0.1 M PB (pH 7.3). The right half of each segment was then fixed in 1% osmium tetroxide in 0.1 M PB (pH 7.3) followed by dehydration through a graded ethanol series and embedded in Epon 812. Sections (1 μm thick) were cut, stained with toluidine blue, and then examined with the aid of a light microscope.

Photographs (x200) were taken at three points in both the ALF and l-CST. The ALF was divided anteriorly into three equal parts from the medial to lateral margins of the anterior horn and photographs of the mid-medial, mid-lateral and lateral portions were taken (Fig. 2). Large bundles of myelinated fibers with diameters of 10-12 μm (thought to be the intramedullary portion of the anterior spinal root) crossing the ALF were avoided when taking the photographs. The l-CST was divided into four equal parts and photographs were taken at positions midway between the three dividing lines (mid-medial, medial and mid-lateral portions). Enlarged prints (x2285) were made and the mean diameter of the myelinated fibers was obtained, using a digitizer, by averaging the longest and shortest diameters (the latter was perpendicular to the former).

In the present study, in order to determine the origin of the large myelinated fibers in the ALF of the human spinal cord, the number of which is severely reduced in patients with ALS, myelinated fibers in the ALF of the mid-cervical spinal cord were examined quantitatively in five groups of subjects, including control subjects (Group I). The disease

groups that were examined included patients with cerebral lesions showing complete degeneration of the unilateral/bilateral pyramis of the medulla oblongata (Group II), those with lesions of the pontine tegmentum (Group III), those with lesions of the lower cervical spinal cord (Group IV), and those with thoracic/lumbar lesions (Group V) (Fig. 3).

The data for the three areas in the ALF and l-CST of each patient and control subject were summed, and the frequency distribution of the myelinated fiber diameters, in 1-μm increments, was determined and represented on bar charts as the number of myelinated fibers (n) x πr^2 (r: half the mean diameter of the myelinated fibers), to show that the large myelinated fibers, although fewer in number, cover a wide area. The total area of the ALF and of the l-CST in each patient examined was 0.057 mm^2. For the control subjects, the average of each increment was expressed on the bar chars, and for the ALS cases, the data obtained for each patient and the average values for the patients with and without respirator-support were evaluated. Statistical evaluation was performed using the Mann-Whitney U test to compare the number of myelinated fibers with diameters of less than 3 μm (small), 3-6 μm (medium), and over 6 μm (large).

The myelinated fibers in the ALF and l-CST were quantitatively examined bilaterally in control subjects and in patients with cerebral lesions. Based on the obtained data that there was no difference in number between the myelinated fibers in the right and left side, those in the right side of the ALF and l-CST were examined in other groups.

ANATOMIC DEFINITION OF NERVE FIBER TRACTS IN THE SPINAL CORD

The white matter of the spinal cord contains bundles of various nerve fiber tracts. It has been reported that the anterolateral funiculus (ALF), which is the ventral part of the lateral funiculus [Nathan et al. 1996], contains, as long-descending tracts, the ventral pyramidal tract (human [Barnes 1901]), corticospinal tracts (human [Nathan et al. 1990]), reticulospinal tracts (cat, opossum and human [Ikuta et al, 1982, Iwamoto et al. 1990, Martin et al. 1979, Nathan et al. 1996, Nyberg-Hansen 1965, Parent 1996]), the vestibulospinal tract (cat and human [Parent 1996, Rose et al. 1996, Shinoda et al. 33]), and raphe spinal tracts (opossum [Martin et al. 1982]). In addition, the ALF contains, as long-ascending tracts, the spinothalamic tract (human [Kuru 1976, Parent 1996, Smith 1951, Smith 1957]), the spinoreticular tract (human [Parent 1996]), the spinocerebellar tract (human [Kuru 1976, Parent 1996]), and Helweg's triangular tract (human [Smith & Deacon 1981]). Propriospinal fibers (cat and human [Altermark et al. 1987, Giok 1958, Parent 1996]) have also been observed.

On the origin of these fibers, experimental studies of animals and human autopsy cases with various destructive lesions in the brain and spinal cord revealed the topographic localization of the neurons, however, the origin neurons of the above mentioned nerve tracts have not yet been completely ascertained in humans so far (Fig. 1).

LATERAL CORTICOSPINAL TRACT (l-CST) DEGENERATION AND SPINAL NEURON LOSS

Patients with ALS of long course of the illness or on artificial respiration usually

show severe loss of neurons in the spinal gray matter including anterior horn and intermediate zone (Fig. 4 & 5). On the contrary, the spinal cord of a housewife, who died at the age of 59 with 1 year-7 months-clinical course refusing the use of a respirator, and whose muscular strength was fairly well preserved up to death, shows only moderate loss of AHCs and quite well preserved neurons in the intermediate zone (Fig. 6). The findings indicate that the primary degeneration may occur in the AHCs and the neurons in the intermediate zone degenerate sequentially in the spinal gray matter in ALS (Fig. 7).

These findings indicate the occurrence of a sequential degeneration of the neurons in the intermediate zone (Rexed's [Rexed 1954] laminae V-VIII) of the spinal cord to loss of anterior horn cells (Rexed's lamina IX) in patients with ALS [Oyanagi et al. 1983, 1989]. Terao et al. [1994] also reported neuronal loss in the intermediate zone of the ALS spinal cord. Long-ascending neurons [Parent 1996], internuncial neurons [Parent 1996], and propriospinal neurons [Altermark et al. 1987, Molenaar & Kuypers 1978] have been shown to originate in the intermediate zone of the spinal cord.

It has been reported that the degeneration of the CST caused by hemispherectomy [Ikuta et al. 1982] and stroke [Terao et al. 1997] does not induce trans-synaptic degeneration in the AHCs in humans. Long duration of the illness and respirator use tend to cause severe degeneration of both the l-CST and marked loss of neurons in the spinal gray matter in many patients. However, some patients with marked loss of spinal neurons show relatively mild degeneration of the l-CST (Fig. 8). Based on these findings, the degree of myelinated fiber loss in the l-CST did not completely correlate with either the duration of their illness or their history of respirator use [Oyanagi et al. 1995]. These

findings mean absence of direct correlation of disease mechanism between the AHCs and the l-CST in ALS.

LATERALITY OF CORTICOSPINAL TRACT (CST) DEGENERRATION IN ALS: PROPORTION OF CROSSED AND UNCROSSED FIBERS

Symptoms of most of the ALS patients occurs in unilateral extremity at the initiation. According to the course of the disease, muscle weakness usually progressed to the other extremity in the patients, and the neuropathological examination reveals symmetric or almost symmetric degeneration of the CST and loss of AHCs. However, occasionally, there have been reported asymmetric degeneration of the l-CST [Reuter 1931, Swash et al. 1988] and loss of AHCs [Mochizuki et al. 1995].

The proportion of the crossed (lateral) and uncrossed (anterior) CST should be considered, when asymmetric degeneration of the CST is present in the spinal cord, since dysproportion, probably developmental, of the crossed and uncrossed CST is observed occasionally in Japanese subjects in routine neuropathological examination. It has been observed that the apparent asymmetry of the CST degeneration was caused not by the severity of the degeneration, but by the dyspropotion of the nerve fibers of the crossed and uncrossed CST (Fig. 9).

LOSS OF MYELINATED FIBERS IN THE ANTEROLATERAL FUNICULUS (ALF) IN CLASSIC ALS

In the white matter of most the patients with sporadic ALS, the ALF degenerates

along with the lateral and anterior CST [Charcot 1880, Holmes 1909, Ikuta et al. 1979, 1982, Lawyer & Netsky 1953, Oyanagi et al. 1995, Smith 1960]. In the present morphometric study on the myelinated fibers in the ALF and l-CST of the cervical segment revealed that: (1) marked and significant loss of large myelinated fibers in the ALF of ALS patients, (2) the patients who required respirator support showed more severe degeneration of the ALF in the ALS than those who required none, and (3) the degree of myelinated fiber loss in the l-CST did not correspond with either the illness duration or the history of respirator use, (4) large myelinated fibers in the l-CST and ALF degenerate independently in classic ALS [Oyanagi et al. 1995] (Fig. 10).

ORIGIN OF THE DEGENERATED FIBERS OF THE ALF IN CLASSIC ALS

The neurons originating the reticulospinal tract, the neurons in the spinal cord [Ikuta et al. 1982], and the propriospinal neurons [Oyanagi et al. 1983, 1989] have been proposed as the origins of the degenerated fibers observed in the ALF of patients with ALS.

In the present study, in order to determine the origin of the large myelinated fibers in the ALF of the human spinal cord, the number of which is severely reduced in patients with ALS, myelinated fibers in the ALF of the mid-cervical spinal cord were examined quantitatively in five groups of subjects, including control subjects (Group I). The disease groups that were examined included patients with cerebral lesions showing complete degeneration of the unilateral/bilateral pyramis of the medulla oblongata (Group II), those with lesions of the pontine tegmentum (Group III), those with lesions of the lower

cervical spinal cord (Group IV), and those with thoracic/lumbar lesions (Group V) (Fig. 3).

The results of the present study have revealed that: (1) large myelinated fibers in the ALF of the mid-cervical spinal cord originate from the tegmentum of the brain stem and from the lower cervical spinal cord, (2) large and medium-sized myelinated fibers in the ALF of the mid-cervical spinal cord are not corticospinal tracts, (3) nor are these fibers long-ascending tracts from the thoracic and lumbar spinal cord (Table 1).

A histological and quantitative study has revealed neither degenerative fibers, loss of myelinated fibers, nor atrophy of the ALF in patients with hemispherectomy [Ueki 1966]. The finding concurs with the results of the present study.

The number of large and medium-sized myelinated fibers in the ALF of the mid-cervical spinal cord in patients with complete transverse myelopathy at the thoracic level was not reduced. This indicates that the long-ascending tracts, such as the spinothalamic [Kuru 1976, Parent 1996, Smith 1951, Smith 1957], spinoreticular [Parent 1996], spinocerebellar [Kuru 1976, Parent 1996], and Helweg's triangular [Smith & Deacon 1981] tracts are either not composed of large or medium-sized myelinated fibers, or else do not pass through the areas investigated in the present study.

The result of the present study shows that a proportion of the large myelinated fibers in the ALF of the mid-cervical spinal cord originate from the lower cervical cord, and that the large myelinated fibers in the ALF are not long-ascending fibers from the thoracic and lumbar spinal cord. This finding suggests that the large myelinated fibers reduced in number in patients with lower cervical involvement are not long-ascending

fibers, but propriospinal fibers connecting neighboring segments. The present study has also revealed that the large myelinated fibers in the ALF of the mid-cervical segment originate from the tegmentum of the brain stem and the lower cervical spinal cord, and their origins are considered to be reticulo-, vestibulo- and/or raphe-spinal neurons, and propriospinal neurons.

In advanced ALS patients who require the long-term use of a respirator, an extensive reduction in the number of neurons other than motor neurons has been observed in addition to complete loss of the anterior horn cells [Hayashi & Kato 1989, Mizutani et al. 1992]. It has also been noted that the tegmentum of the brain stem and the intermediate zone of the spinal cord exhibit extremely severe atrophy and neuronal loss, and that the ALF degenerates markedly in these ALS patients [Hayashi & Kato 1989, Mizutani et al. 1992]. Bunina bodies and ubiqutin-immunopositive inclusions have been observed in the neurons of the reticular formation of the medulla oblongata in patients with ALS [Bergmann 1993, Nakano et al. 1993]. This indicates that an ALS specific disease process exists in the neurons in the reticular formation.

It has been shown that propriospinal neurons at the cervical segment are located in laminae V-VII (cat and monkey [Molenaar and Kuypers 1978]) of Rexed [Rexed 1954], and that these neurons play roles in movement control and sensorimotor integration of the extremities [Martin 1996, Pierrot-Deseilligny 1996]. The reticulospinal and propriospinal tracts terminate in laminae V-VIII in the cervical cord (cat [Barilari & Kuypers 1969]). Thus, the reticulospinal neurons in the brain stem and propriospinal neurons in the spinal cord are considered to be closely linked to the degeneration of the